0944

# THEORETICAL CRACK ANGLE IN REINFORCED CONCRETE ELEMENTS SUBJECTED TO STRONG EARTHQUAKES

**Jang Hoon KIM[1] And John B MANDER[2]**

## SUMMARY

The purpose of this paper is to develop a mathematical expression for computing crack angles based on reinforcement volumes in the longitudinal and transverse directions, member end-fixity and length-to-width aspect ratio. For this a reinforced concrete beam-column element is assumed to possess a series of potential crack planes represented by a number of differential truss elements. Depending on the boundary condition, a constant angle truss or a variable angle truss is employed to model the cracked structural concrete member. The truss models are then analyzed using the virtual work method of analysis to relate forces and deformations. Rigorous and simplified solution schemes are presented. An equation to estimate the theoretical crack angle is derived by considering the energy minimization on the virtual work done over both the shear and flexural components of truss models. The crack angle in this study is defined as the steepest one among fan-shaped angles measured from the longitudinal axis of the member to the diagonal crack. The theoretical crack angle predictions are validated against experimentally observed crack angle reported by previous researchers in the literature. Good agreement between theory and experiment is obtained.

## INTRODUCTION

When reinforced concrete structures are subjected to large deformation reversals due to strong earthquake loading, structural damage starts with cracking. The critical strength mechanism, governed by either shear or flexure, is determined not only by the reinforcing steel layout, but also by the nature of the crack formulation, particularly the crack pattern and angles. The crack angle in a structural concrete member is very important as it affects the post-cracking stiffness as well as the ultimate strength of the member. Recent research in the United States, and elsewhere, has proposed analysis and design models for the seismic shear strength of reinforced concrete column members, explicitly or implicitly, with reference to a critical crack angle [ACI, 1995; AASHTO, 1994; Eurocode, 1991; Collins and Mitchell, 1991; Hsu, 1993; Priestley, et al., 1994a,b]. For example, the steel component of shear resistance is given, in its most general form, by

$$V_s = A_{sh} f_{yh} \frac{jd}{s} \cot\theta \quad (1)$$

where $A_{sh}$ = section area of shear steel, $f_{yh}$ = yield strength of shear steel, $jd$ = internal lever arm, $s$ = transverse hoop spacing and $\theta$ = crack angle. But no guidance is given to designers as to the variability of this important parameter. Rather, engineers are required to use prescribed values—for example 30 and 35 degrees for analysis and design, respectively—regardless of the reinforcement configuration and/or aspect ratio [Priestley, et al., 1994a,b]. These arbitrary values for crack angles have been based on empirical observations, but not sound theory. Therefore, a mathematical expression for computing crack angles is developed in the present paper based on reinforcement volumes in the longitudinal and transverse directions, member end-fixity and length-to-width aspect ratio.

*[1] Department of Architecture, Ajou University, Suwon 442-749, South Korea Email: kimjh@madang.ajou.ac.kr*
*[2] Dept of Civil Engineering, State University of New York at Buffalo, NY 14260, U.S.A.Email: jmander@acsu.buffalo.edu*

## TRUSS MODELING OF CRACKED CONCRETE ELEMENTS

It has long been recognized that the behavior of reinforced concrete beam-columns after onset of cracking can be analyzed using an appropriate truss model. In truss analogy, longitudinal reinforcement is represented by longitudinal chords of a truss, while transverse hoop steel is represented by transverse tensile ties. The effect of concrete in flexural compression may be considered as a part of the longitudinal compression chord member. The longitudinal chords and the transverse tensile ties are assumed to be internally stabilized by the struts that model concrete regions under compression in the diagonal direction. The inclination of the diagonal struts should coincide with the probable diagonal crack direction. For simplicity, the longitudinal chords, transverse tensile ties and diagonal struts are assumed to be joined together through rigid nodes. Schlaich, et al.[1987] defined two standard regions in structural concrete elements depending on the complexity of stress distribution: undisturbed (B-) and disturbed (-D) regions. The definition is used through this paper.

### Constant Angle Truss

The shear transfer mechanism for undisturbed regions in a diagonally cracked long beam-column member is shown in figure 1. From the overall member shown in figure 1(a), a differential portion of truss with prismatic members having finite depths can be extracted for analysis purpose as shown in figure 1(b). In this representation, it is assumed that the transverse steel is uniformly distributed over the length of the member. Now, consider this single differential truss subjected to the differential shear force $dV_s$. Member forces of the differential truss can be easily found by the static equilibrium. The shear deformation of a differential truss can then be calculated using the principle of Virtual Work. Rigid longitudinal chords are assumed in order to negate the effect of flexural deformation. It is noted that under constant shear, the deformation of each differential truss is the same over the entire constant angle truss. The shear stiffness of the entire cracked concrete member due to constant angle truss mechanism is obtained by carrying out the integration over the length defined by crack angle, $jd\cot\theta$. That is,

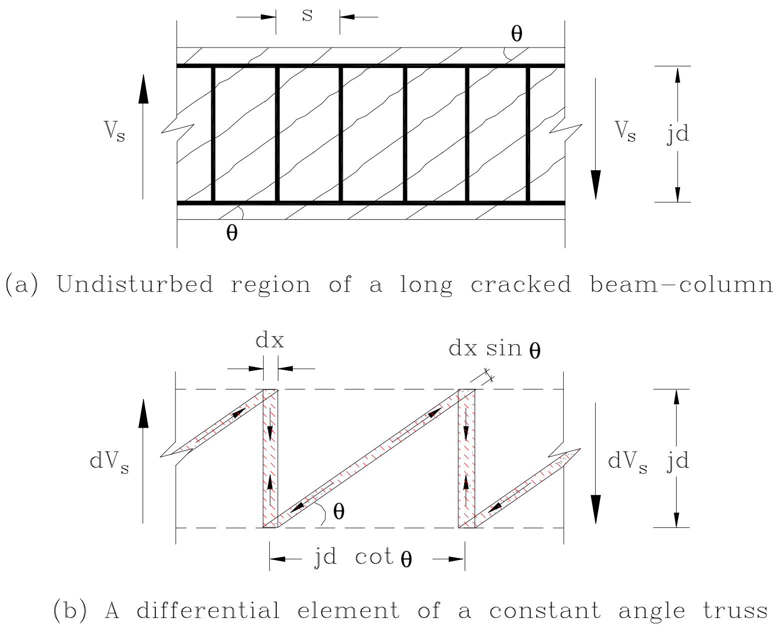


**Figure 1: Constant angle truss model**

$$K_s = \int dK_s = \int \frac{dV_s}{\Theta_s} = \frac{\rho_v n \cot^2\theta}{1+\rho_v n \operatorname{cosec}^4\theta} E_c A_v \tag{2}$$

where $\Theta_s$ = drift angle due to shear, $\rho_v$ = volumetric ratio of shear steel, $n = E_s / E_c$ = modulus ratio, $E_c$ = modulus of elasticity of concrete, $E_s$ = modulus of elasticity of steel and $A_v$ = shear area of concrete section.

**Variable Angle Truss**

The variable angle truss can approximately represent a diagonally cracked short column where disturbed regions prevail as shown in figure 2(a). Consider a single differential truss element subjected to $dV_s$ in figure 2(b). But $dV_s$ is not uniform through the length at this time. Note that a differential truss consists of a steel tie with depth $Ldx$ and two tapered diagonal struts, where $x$ is a non-dimensional parameter varying from 0 through 1. A tapered strut is idealized as a prismatic one with average depth. In a manner similar to the solution of the constant angle truss mechanism, the elastic shear stiffness of a cracked concrete column is obtained by integrating the differential stiffness over the entire length, thus

$$K_s = \int dK_s = \int_0^1 \frac{\rho_v n E_c A_v \cot^2\alpha}{1 + 2\rho_v n\left[\left\{1 + x^2\cot^2\alpha\right\}^{\frac{3}{2}} + \left\{1 + (1-x)^2\cot^2\alpha\right\}^{\frac{3}{2}}\right]}\,dx \tag{3}$$

where $\alpha$ = corner-to-corner diagonal angle. Since a closed-form analytical solution to this equation has not found, an appropriate numerical integration scheme is used instead. Then equation (3) can be expressed as

$$K_s = \sum_{i=1}^{N} \frac{\omega_i \rho_v n \cot^2\alpha}{1 + 2\rho_v n\left[\left\{1 + x_i^2\cot^2\alpha\right\}^{\frac{3}{2}} + \left\{1 + (1-x_i)^2\cot^2\alpha\right\}^{\frac{3}{2}}\right]}\,E_c A_v \tag{4}$$

in which $N$ = number of numerical integration points, $\omega_i$ = weight factor at $i^{th}$ point, $x_i$ = normalized coordinate

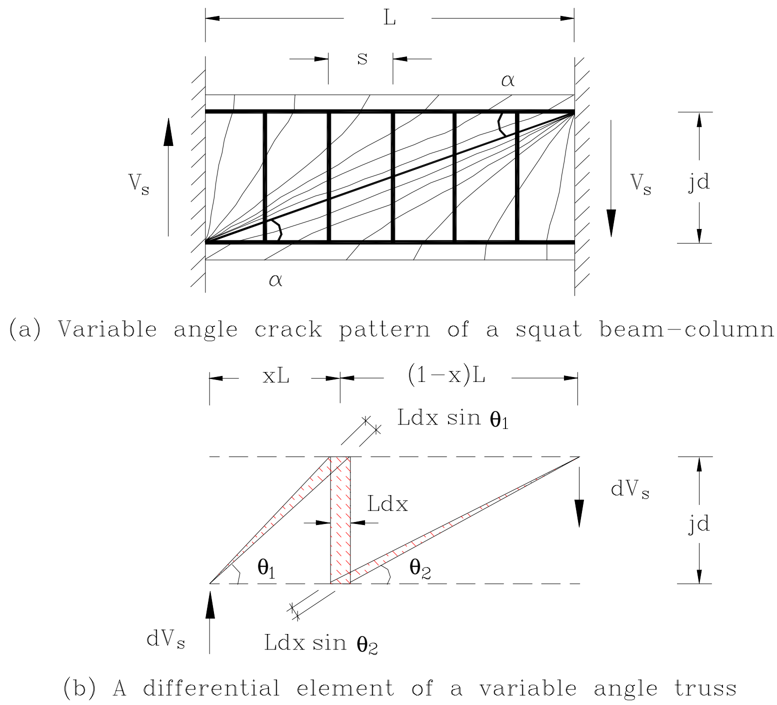


**Figure 2: Variable angle truss model**

of $i^{th}$ numerical point. Any numerical integration scheme such as two-point and three-point Gauss quadratures, Trapezoidal rule, Simpson's 1/3 rule and Boole's rule may be used for solving equation (4). It should be noted that for squat columns where shear is generally critical (small $L / jd$ ), there is virtually no difference in stiffness calculations between numerical schemes as shown in figure 3. Since equation (4) with numerical parameter values is lengthy, a convenient simplified solution can be used as

$$K_s = \frac{\rho_v n \cot^2 \alpha}{1 + 4\rho_v n \left(1 + 0.39 \cot^2 \alpha\right)^2} E_c A_v \qquad (5)$$

The cracked elastic shear stiffness calculated by this approximation is favorably compared to the exact one in figure 4, where Simpson's 1/3 rule with $N = 20$ is regarded as exact.

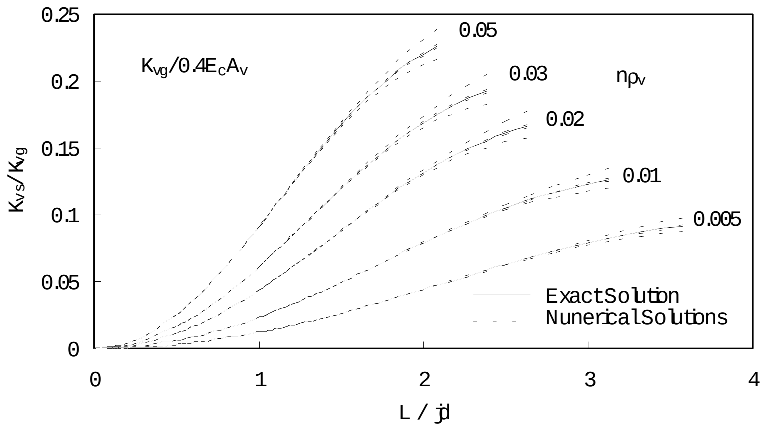


**Figure 3: Comparison of shear stiffnesses between numerical schemes**

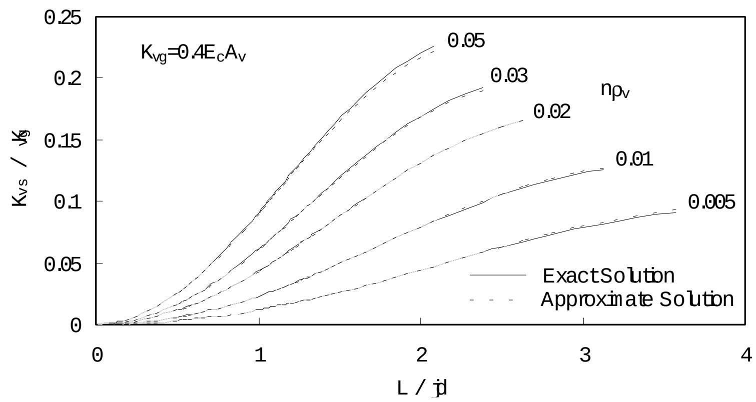


**Figure 4: Approximation of shear stiffness due to variable angle truss**

## COMPARISON OF STIFFNESSES

Figure 5 compares the stiffness of constant angle truss given by equation (2) with the exact one of the variable angle truss given by equation (4). For this purpose, it is necessary to put $\alpha = \theta$ which denotes that the steepest crack angle to the longitudinal axis of the fan-shaped cracks at disturbed region of the column will be equal to the constant crack angle at undisturbed region. Note that there is no remarkable difference between constant angle truss and variable angle truss, and any model can be used for determining shear stiffness over the length of the member.

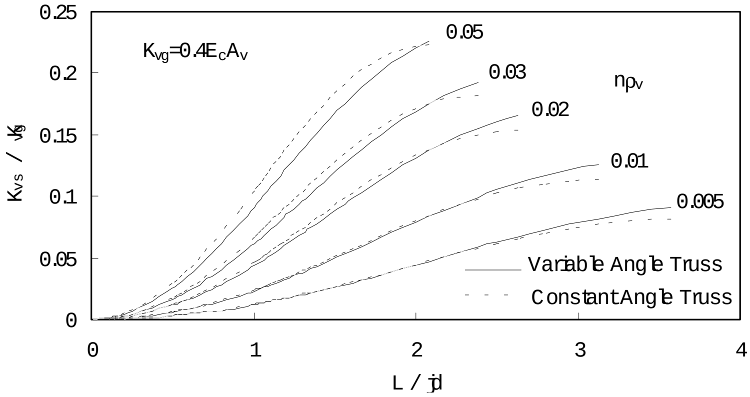


**Figure 5: Comparison of shear stiffness between truss models**

### Two-Point Gauss Truss Model

Using equation (4) with numerical integration weights, the variable angle truss model in figure 2 can be physically simplified with reasonable accuracy. Implementation of Gauss quadrature with two points results in the two-point Gauss truss model as shown in figure 6. Axial rigidities of truss members at i^th numerical point are given by

$$(EA)_{Ti} = \omega_i E_s A_{sh} \frac{L}{s} \tag{6}$$

$$(EA)_{di} = \frac{0.5\omega_i}{\sqrt{x_i^2 + \tan^2\alpha}} E_c A_v \tag{7}$$

$$(EA)_L = 0.5 E_s A_{st} = 0.5 E_c A_g \rho_t n \tag{8}$$

where $\omega_1 = \omega_2 = 0.5$, $x_1 = 0.2113249$, $x_2 = 0.7886751$, $A_{st}$ = section area of longitudinal steel, $A_g$ = gross section area of concrete element and $\rho_t = A_{st} / A_g$. It is noted that the strut section area in equation (7) can also be obtained by measuring the depth of diagonal struts along the truss center line on the scaled sketch.

The shear deformation of the truss model is determined using the Virtual Work method of analysis on the transverse ties and diagonal struts. Thus the shear stiffness of the truss models with fixed-fixed and fixed-pinned ends should be the same. The flexural deformation of the truss model can be determined also using the Virtual Work method of analysis considering only the longitudinal chord members. The elastic flexural stiffness of a cracked concrete column about drift angle due to the variable angle truss model is given by

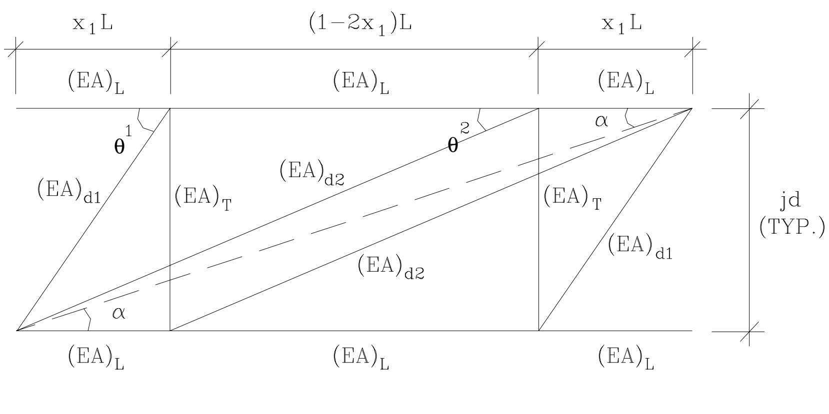


**Figure 6: Truss model by two-point Gauss quadrature**

$$K_f = \frac{E_s A_{st}}{\varsigma \cot^2 \alpha} \tag{9}$$

where $\varsigma = 0.5704$ for fixed-fixed end and $\varsigma = 1.5704$ for fixed-pinned end.

## DETERMINATION OF CRACK ANGLE

It is believed in this study that the crack angle in a concrete member depends on both shear and flexural components of displacement and will occur at an orientation that requires the minimum amount of energy.

### Energy Consideration

The external work done on the structural member due to unit shear force ($V_s = 1$) is the same as the total drift angle, thus using equations (2) and (9)

$$EWD = \Theta_1 = \Theta_{s,1} + \Theta_{f,1} = \frac{1 + \rho_v n \operatorname{cosec}^4\theta}{E_c A_v \rho_v n \cot^2\theta} + \frac{\varsigma \cot^2\theta}{E_c A_g \rho_t n} \tag{10}$$

Minimizing the external work done by differentiating equation (10) with respect to $\theta$ leads to the crack angle causing the minimum energy, that is

$$\frac{d(EWD)}{d\theta} = 0 \tag{11}$$

which has a solution

$$\theta = \tan^{-1}\left(\frac{\rho_v n + \varsigma \frac{\rho_v}{\rho_t} \frac{A_v}{A_g}}{1 + \rho_v n}\right)^{\frac{1}{4}} \tag{12}$$

### Experimental Validation

Table 1 presents a comparison of twenty experimentally observed crack angles with those computed using equation (12). The comparison is also made in figure 7 by visualizing the data in table 1. It is evident that the theoretical results compare very favorably with the experimentally observed crack angles. This clearly shows the dependence of the crack angle on the quantity of longitudinal as well as transverse reinforcement.

## CONCLUSIONS

Cracked structural concrete elements are modeled by considering postulated crack planes resulting in either of a constant angle truss or a variable angle truss. Both truss models are satisfactory for determining the shear stiffness over the length of the beam-column. It is shown that numerical integration schemes can be implemented for physical simplification of the truss model. A theoretical foundation for computing the principal crack angle is formulated using energy considerations. Therefore, it is concluded that the crack angle of 45° that has been traditionally assumed in ACI 318 code [1995] for many decades as well as the newly suggested 30° recommended by Priestley, et al. [1994a,b] both leads to a faulty prediction of shear strength.

**Table 1: Comparison of crack angles between theory and experiment**

| Specimen | Boundary | n | $\rho_t$ | $\rho_v$ | $A_v / A_g$ | $\theta_{theory}$ | $\theta_{\exp}$ |
|---|---|---|---|---|---|---|---|
| 1/3 Model Pier[a] | F-F | 5.7 | 0.0186 | 0.00147 | 0.756 | 24.3° | 26° |
| Prototype[a] | F-P | 6.3 | 0.0186 | 0.00115 | 0.746 | 27.9° | 26° |
| 1/3 Model[b] | F-P | 6.0 | 0.0102 | 0.00492 | 0.701 | 40.7° | 39° |
| Column A[c] | F-P | 7.8 | 0.0156 | 0.00785 | 0.405 | 37.8° | 36° |
| Column C[c] | F-P | 7.9 | 0.0156 | 0.01178 | 0.405 | 40.4° | 39° |
| Column D[c] | F-P | 7.9 | 0.0156 | 0.00785 | 0.405 | 37.8° | 33° |
| Circular C1[d] | F-F | 7.2 | 0.0254 | 0.00089 | 0.852 | 21.3° | 22° |
| Rectangular R2[d] | F-F | 7.2 | 0.0255 | 0.00102 | 0.901 | 22.2° | 23° |
| Unit 9[e] | F-P | 7.8 | 0.032 | 0.00518 | 0.828 | 35.0° | 35° |
| Unit 13[e] | F-P | 7.1 | 0.032 | 0.00518 | 0.828 | 34.9° | 35° |
| Unit 14[e] | F-P | 7.3 | 0.0324 | 0.00259 | 0.828 | 30.5° | 31° |
| Unit 16[e] | F-P | 7.4 | 0.032 | 0.00259 | 0.828 | 30.6° | 32° |
| 2R10-60u[f] | F-P | 7.8 | 0.032 | 0.00727 | 0.81 | 37.1° | 38° |
| 4R6-65u[f] | F-P | 7.8 | 0.032 | 0.00239 | 0.828 | 30.1° | 26° |
| 4R10-60u[f] | F-P | 7.8 | 0.032 | 0.00727 | 0.81 | 37.1° | 36° |
| 0R6-80b[f] | F-P | 7.8 | 0.032 | 0.00194 | 0.828 | 28.9° | 29° |
| 2R6-60b[f] | F-P | 7.8 | 0.032 | 0.00259 | 0.828 | 30.6° | 30° |
| R1A[g] | F-F | 6.9 | 0.025 | 0.00123 | 0.881 | 23.0° | 24° |
| R3A[g] | F-F | 7.2 | 0.025 | 0.00123 | 0.881 | 23.1° | 24° |
| R5A[g] | F-F | 7.5 | 0.025 | 0.00123 | 0.881 | 23.1° | 22° |

[a]Pier circular column with retrofitted beam-column joints [Mander, et al., 1996a,b]
[b]Seismically designed circular column [Mander and Cheng, 1995]
[c]Square hollow-core columns [Mander, et al., 1984]
[d]Columns[Chai, et al., 1990]
[e]Circular columns [Ang, et al., 1989]
[f]Circular columns [Wong, 1990]
[g]Rectangular columns [Priestley, et al., 1994a,b]
F-F: Fixed-fixed ends
F-P: Fixed-pinned ends

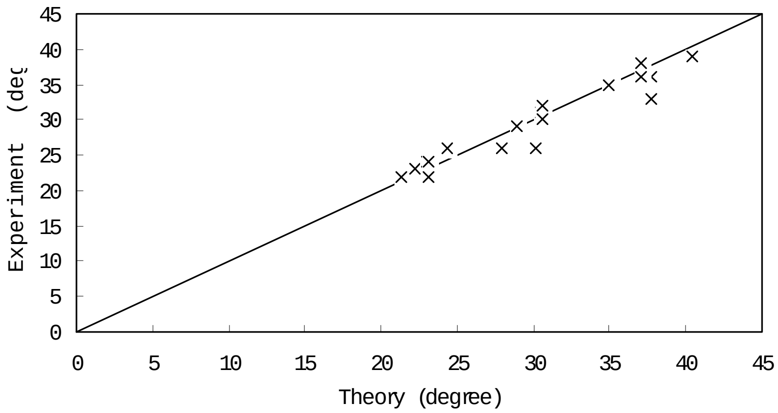


**Figure 7: Crack angle comparison between theory and experiment**

## REFERENCES


AASHTO (1994), *LRFD Bridge Design Specifications*, 1st ed., American Association of State Highway and Transportation Officials, Washington, D.C.

ACI Committee 318 (1995), *Building Code Requirements for Structural Concrete and Commentary*, American Concrete Institute, Detroit.

Ang, B.G., Priestley, M.J.N. and Paulay, T. (1989), "Seismic Shear Strength of Circular Reinforced Concrete Columns", ACI Structural Journal, Title No. 86-S6, Jan.-Feb., pp. 45-59.

Chai, Y.H., Priestley, M.J.N. and Seible, F. (1990), "Retrofit of Bridge Columns for Enhanced Seismic Performance", *Proceedings of the First U.S.-Japan Workshop on Seismic Retrofit of Bridges*, Public Works Research Institute, Tsukuba, Japan, pp. 321-340.

Collins, M.P and Mitchell, D. (1991), *Prestressed Concrete Structures*, Prentice-Hall, Inc.

Eurocode No. 2 (1991), *Design of Concrete Structures, Part 1: General Rules and Rules for Buildings*, Thomas Telford, London.

Hsu, T.T.C. (1993), *Unified Theory of Reinforced Concrete*, CRC Press, Inc.

Mander, J.B., Priestley, M.J.N. and Park, R. (1984), *Seismic Design of Bridge Piers*, Research Report No. 84-2, University of Canterbury, New Zealand.

Mander, J.B. and Cheng, C.-T. (1995), "Renewable Hinge Detailing for Bridge Columns", *Proceedings of Pacific Conference on Earthquake Engineering*, Australia, November 20-22, pp. 197-206.

Mander, J.B., Mahmoodzadegan, B., Bhadra, S. and Chen, S.S. (1996a), *Seismic Evaluation of A 30-Year Old Non-Ductile Highway Bridge Pier and Its Retrofit*, Technical Report NCEER-96-0008, National Center for Earthquake Engineering Research, State University of New York at Buffalo, New York.

Mander, J.B., Kim, J.H. and Ligozio, C.A. (1996b), *Seismic Performance of A Model Reinforced Concrete Bridge Pier Before and After Retrofit*, Technical Report NCEER-96-0009, National Center for Earthquake Engineering Research, State University of New York at Buffalo, New York.

Preistley, M.J.N., Seible, F., Xiao, Y. and Verma, R. (1994a), "Steel Jacket Retrofitting of Reinforced Concrete Bridge Columns for Enhanced Shear Strength – Part 1: Theoretical Considerations and Test Design", *ACI Structural Journal*, Vol. 91, No. 4, July-August, pp. 394-405.

Preistley, M.J.N., Seible, F., Xiao, Y. and Verma, R. (1994b), "Steel Jacket Retrofitting of Reinforced Concrete Bridge Columns for Enhanced Shear Strength – Part 2: Test Results and Comparison with Theory", *ACI Structural Journal*, Vol. 91, No. 5, September-October, pp. 537-551.

Schlaich, J., Schafer, K. and Jennewein, M. (1987), "Toward a consistent Design of Structural Concrete", *PCI Journal*, Vol. 32, No. 3, May-June, pp. 74-150.

Wong, Y.L. (1990), *Squat Circular Bridge Piers under Multi-Directional Seismic Attack*, Ph.D. Dissertation, Department of Civil Engineering, University of Canterbury, Christchurch, New Zealand.